S7-020

Properties of M197, M160, M202, L131, and L166 mutants from QM/MM optimized structures of *Rhodobacter Sphaeroides*

N. S. Hush[1,2], J. M. Hughes[1], M. C. Hutter[1], and J. R. Reimers[1]

[1]*School of Chemistry, University of Sydney, NSW 2006, AUSTRALIA.*

[2] *Department of Biochemistry, University of Sydney, NSW 2006, AUSTRALIA.*
Email: hush_n@chem.usyd.edu.au Fax 61-2-93513329

Keywords: special pair, protein structure, hydrogen bonding, midpoint potential, vibrational frequency

1. Orientation of the 2a acetyl groups in the wild type, FY(M197), and FH(197) mutants of the neutral and oxidised reaction centre

The 2a-acetyl groups of the special pair shown in Fig.1 may each be oriented in one of two general directions, either with their oxygen atoms facing inward forming a sixth ligand to the magnesium of the other half, or oriented outwards forming a hydrogen-bond to the surrounding protein. We have calculated [Reimers 1999] that the carbonyl group always twists ca. 40^{o} out of plane for both inward- and outward- pointing structures.

The calculated structures show that in F*x*(M197) mutants a hydrogen bond to the 2a-acetyl group of P_M, is introduced, but we predict that this will not persist following oxidation to form P^+: from model calculations [Reimers 1999] that there is a large driving force for hydrogen bond breakage of ca. 7 kcal mol^{-1} resulting from preference of the Mg in the charged Bchl to coordinate to a carbonyl group rather than to a methyl. This will be sufficient to overcome the hydrogen bonding with the protein.

On the other hand, they show that for HF(L168) mutants, the hydrogen bond is removed on mutation and that the 2a-acetyl of P_L rotates to coordinate to the Mg of P_M. However, in the (oxidized) special-pair radical cation of HF(L168) mutants, a large fraction of the charge is localized on P_M and hence the electrostatic interaction between P_M and the electron-rich carbonyl should be sufficient to guarantee the magnesium-coordinated configuration. By contrast, in the wild type and most other mutants, much less charge is delocalized onto P_M, reducing the attractiveness of the coordinated orientation and the hydrogen bond to P^+ is predicted to remain intact.

2. The structure of the FY(M197) mutant

The FY(M197) mutant has attracted particular attention because its P_M 2a-acetyl frequency is 1636 cm^{-1}, 6 cm^{-1} greater than that of the related FH(M197) mutant. With the aid of X-ray structural information, this has been interpreted in terms of reduced hydrogen-bonding caused by a configuration for the protein which differs from that in either *Rh.Viridis* WT or *Rb. Sphaeroides* wild type and results in a modified hydrogen bonding arrangement. Our results [Hughes 2001] do indeed

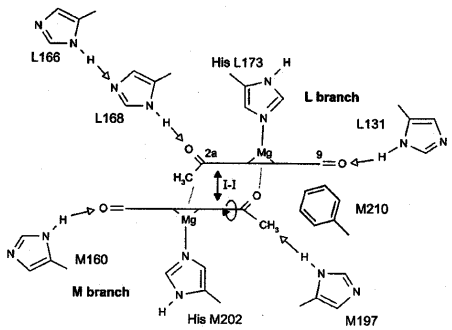

Figure 1 Protein-cofactor interactions

predict the observed alternate configuration in which the aromatic axis in the mutant is oriented differently from the wild types; ***further***, they indicate that the introduced tyrosine has considerable structural flexibility.

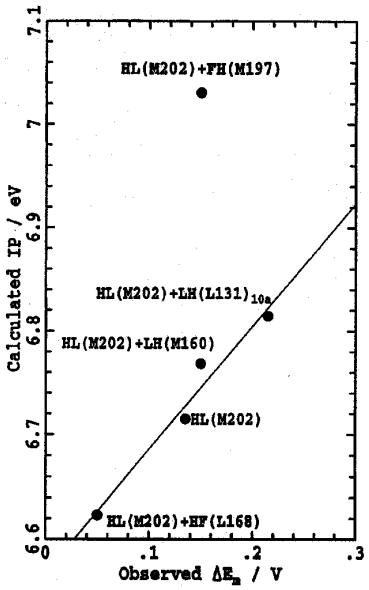

Figure 2 Midpoint potential vs. the calculated ionization energy

3. Water penetration in the oxidized FY(M197) mutant

The M197 residue is located adjacent to the special pair but forms part of the hydrophobic-hydrophilic border within the protein. In the X-ray structure of the wild type, two water molecules are located adjacent to this residue but distant from the special pair. The introduction of tyrosine at M197 offers the possibility of an additional water molecule being drawn to the other side of this reside, near the special pair; such a molecule could form three hydrogen bonds, interacting with asparagine M195, serine M158, and HOH28. In the X-ray structure of the neutral a large void capable of accommodating a water molecule is apparent in this region, and one indeed may be present in the oxidized reaction centre P^+ as it would act to solvate the charge, thus significantly lowering the mid-point potential. Further, as the hydrogen bond from tyrosine M197 to the special pair is expected to be broken in P^+, the tyrosine itself is free to reorient and hence form a *fourth* hydrogen bond with the introduced water. This strongly suggests that water penetration near the oxidized special pair occurrs.

The observed mid-point potential of P in FY(M197) is anomalously low, 0.146 V lower than that in FH(M197). We have calculated a structure for the neutral species of P containing an extra water molecule; this is calculated to lower the potential by 0.10 eV. In addition, reorientation of the OH group of tyrosine M197 towards the introduced water and other structural relaxation effects would be expected to provide an additional lowering of the potential. While speculative, this calculation provides a plausible explanation for the observed highly anomalous potential.

4. Chain distortion in L*x*(M160) mutants

The L*x*(M160) series of mutants have been developed to introduce hydrogen bonds to the 9-keto groups of P_M, and it is clear from spectroscopic evidence that the desired results have indeed been obtained. These mutants have formed an important part of the overall reaction-centre research through correlations which link their special-pair mid-point potentials to fundamental intermolecular interaction properties. However many of these (eg., LS(M160) and LN(M160)) involve the replacement of a large residue with a small one, and if the skeletal backbone remains largely invariant, then for the small residues, no hydrogen bond could form. Displacements of the protein backbone of up to 1.7 Å were required to obtain separations as short as these for LS(M160) and LN(M160) [Hughes 2001]. Smaller changes at much larger distances occur; and if relaxation of the entire helical protein strand and its neighbouring strands is not included in the calculations then the introduced hydrogen bond was always found to break as the protein returned to its original configuration.

5. The mid-point potential of P for the heterodimer (HL(M202)) mutants

The study of the mid-point potentials for the oxidation of P to P^+ has produced valuable information about the interaction between the two BChl molecules in the special pair and the extent of charge localization in the cation. For the heterodimer mutants, the cation is essentially fully charge-localized on P_L and these thus form a chemically simple subset. We have evaluated their ionization energies at the Koopmans' level based on the QM/MM wavefunctions using a new technique: these are shown in Fig. 2 as a function of the observed change in mid-point potential from the wild type, E_m. Four of the five points on this graph fall on a straight line, but the mid-point potential for the fifth mutant, HL(M202)+FH(M197) lies quite dramatically some 0.28 eV above the expected line. We deduce [Reimers 1999] that this arises due to the cleavage of the hydrogen bond between His197 and the 2a-acetyl group of P_M in P^+.

6. Competition for hydrogen bonding to the introduced histidine between the 9-keto and 10a-ester groups in L*x*(M160) and LH(L131) mutants

For LH(L131) mutants, the intended HisL131 hydrogen bond to the 9-keto groups of P_L is not always found. Our results [Hughes 2001] indicate the possibility of alternate hydrogen bonding of HisL131 to the neighbouring 10a-ester of P_L. The mutants HF(L168)+LH(L131) and LH(L131) at 100 K are classified as having the expected hyd-rogen bond while LH(L131) at 15 K, HL(M202)+LH(L131), and FH(M197)+LH(M160)+LH(L131) could be classified as having the alternate structure. Two sets of simulations for the latter group with either bonding pattern gave 10a-ester carbonyl bonded structures stable on the 5 ps timescale except for LH(L131), where the 9-keto H-bond was preferred. The optimized structures are shown in Fig 3. The variation in bonding type is due to fine balancing of the energetics of the 10-a ester rotation, and the reduction in polarity of the P_L 9-keto bond owing to conjugation with the porphyrynic ring, reducing the H-bond strength. The analogous structure obtained for the LH(M160) mutant is also shown in Fig. 3: hydrogen bonding of the histidine to the 10a-ester group is structurally inhibited and hence only hydrogen bonding to the 9-keto group is possible.

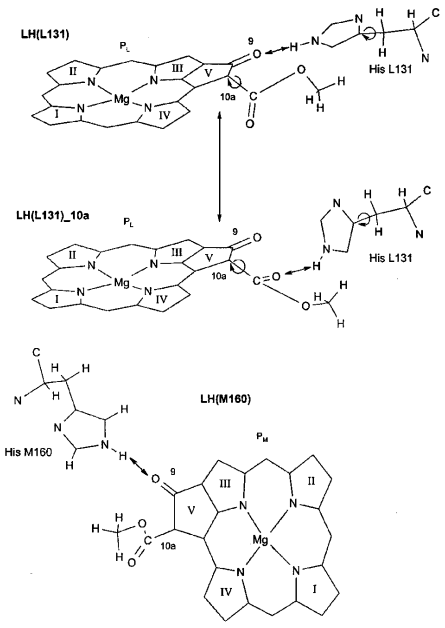

Figure 3 Optimized structures for the introduced histidine in the LH(L131) mutant, showing hydrogen bonding to the 9-keto of PL, its variant LHL(131)_10a in which the hydrogen bonds form to the neighbouring 10a-ester instead, and the analogous bonding in LH(M160)

7. Competitive vs. cooperative hydrogen bonding of HisL168 in N*x*(L166) mutants

The NH(L166) and NL(L166) mutants serve to modify the hydrogen bonding of histidine L168 to the 2a-acetyl group of P_L as suitable residues at site L166 may form an additional hydrogen bond to histidine L168 (see Fig 1). In the wild type, a weak hydrogen bonding ligand, asparagine, is present at L166 while in the mutants either a non-hydrogen-bonding residue, leucine (in NL(L166)), or a strong hydrogen bonding one, histidine (in NH(L166)), is introduced. If cooperative effects are important, then the 2a-acetyl carbonyl frequency should decrease as the L166 to L168 hydrogen-bond strength

increases: a hydrogen bonding residue at L166 would polarize L168 and hence cooperatively increase the strength of the L168 to 2a-acetyl hydrogen bond. However, it was observed that small decreases of the frequency occurred for *both* mutants.

Our simulations indicate that the naive sketch of the structure of the NH(L166) mutant shown in Fig. 1 is highly misleading. The two residues, L166 and L168, are close together, preventing the development of a linear hydrogen-bond such as that sketched in the figure. The NH(L166) and NL(L166) mutants are found to be similar in that neither mutation leads to formation of a hydrogen bond between L166 and L168. Alternatively, the WT clearly does have such a hydrogen bond, with calculated bond lengths of ca. 1.9 Å and hydrogen-bond angles in excess of 140°.

The experimental observation that both mutants have slightly *lower* frequencies than the wild type shows that the cooperative model for frequency modulation is incomplete. Calculated hydrogen bond lengths show that the hydrogen bond between L166 and L168 present in the wild type is thus seen to act *in competition* to the L168 to 2a-acetyl hydrogen bond. Such competitive hydrogen bonding would lead to the hydrogen-bonded species having higher vibration frequencies, as observed.

8. Conclusions

We have constructed representative structures for some 22 reaction centres of mutant strains of *Rh. sphaeroides* and used these to interpret a large range of experimental observations, drawing conclusions about the nature of the wild type and the effects of the introduced mutations. For the two mutants studied for which X-ray structural data is available, good overall agreement between the key qualitative features of the calculated and observed structures is found. All structures correlate well with observed carbonyl frequency changes caused by the mutations, and we find physical causes for unexpected observed frequencies. Also, we demonstrate that, for simple systems in which the location of the hole in P^+ is known *a priori*, these structures alone can be used to interpret changes in observed mid-point potentials thus isolating important chemical effects. A number of other features have also been elucidated. To facilitate other such investigations of the properties of the cofactors using electronic structure techniques, all optimized coordinates have been made available [Hughes 2001].

9. Acknowledgments

We thank the Australian Research Council for funding this research, and Dr. Günter Fritzsch and Dr. Andreas Kuglstatter from the Max-Planck Institute for Biophysics (Frankfurt) for kindly providing us with coordinates from the X-ray structure of FY(M197).

10. References

[Hughes 2001]J.M. Hughes, M.C. Hutter, J.R. Reimers, N.S. Hush *J. Am. Chem. Soc.* **2001**, in press.

[Reimers 2000] J.R. Reimers, M.C. Hutter, J.M. Hughes, N.S. Hush *Int. J. Quant. Chem.* **2000**, *80*, 1224.